Peer-reviewed version available at *Int. J. Mol. Sci.* **2018**, *19*, 2368; doi:10.3390/ijms19082368

Article

Hydrogen Sulfide-Releasing Fibrous Membranes: Potential Patches for Stimulating the Human Stem Cells Proliferation and Viability Under Oxidative Stress.

Ilaria Cacciotti[1,2,3*], Matteo Ciocci[4], Emilia Di Giovanni[4], Francesca Nanni[3,5] and Sonia Melino[3,4*]

1 Department of Engineering, University of Rome "Niccolò Cusano", via Don Carlo Gnocchi 3, 00166-Rome, Italy; ilaria.cacciotti@unicusano.it
2 Italian Interuniversity Consortium on Materials Science and Technology (INSTM), Italy;
3 CIMER Center for Regenerative Medicine, University of Rome Tor Vergata, via Montpellier 1, 0166-Rome, Italy;
4 Department of Chemical Science and Technologies, University of Rome "Tor Vergata", via della Ricerca Scientifica1, 00133-Rome, Italy; melinos@uniroma2.it
5 Enterprise Engineering Department, Italy. University of Rome "Tor Vergata", via del Politecnico 1, 00133-Rome, Italy; fnanni@ing.uniroma2.it

* Correspondence: Sonia Melino e-mail: melinos@uniroma2.it; Tel. #39-0672594410; Ilaria Cacciotti e-mail: ilaria.cacciotti@unicusano.it

Abstract: The design of biomaterial platforms able to release bioactive molecules is mandatory in tissue repair and regenerative medicine. In this context, electrospinning is a user-friendly, versatile and low-cost technique, able to process different kinds of materials in micro- and nano-fibers with a large surface area-to-volume ratio for an optimal release of gaseous signalling molecules. Recently, the antioxidant and anti-inflammatory properties of the endogenous *gasotramsmitter* hydrogen sulfide (H_2S), as well as its ability to stimulate relevant biochemical processes on the growth of mesenchymal stem cells (MSC), have been investigated. Therefore, in this work, new poly(lactic) acid fibrous membranes (PFM), doped and functionalized with H_2S slow-releasing donors extracted from garlic, were synthetized. These innovative H_2S-releasing mats were characterized for their morphological, thermal, mechanical and biological properties. Their antimicrobial activity and effects on the *in vitro* human cardiac MSC growth, either in the presence or in the absence of oxidative stress, were here assessed. On the basis of the results here presented, these new H_2S-releasing PFM could represent promising and low-cost scaffolds or patches for biomedical applications in tissue repair.

Keywords: PLA fibers, organosulfur compounds, garlic extracts, mesenchymal stem cells, microstructure, thermal and mechanical properties, cytotoxicity, antibacterial properties.

1. Introduction

One of the main targets of regenerative medicine is the emulation of the physiological environment by fine-tuning of an array of biochemical and physical stimuli in order to improve stem cells proliferation and differentiation. Many factors with the ability to affect the biological mechanisms of stem cells have already been identified, due to their potential relevance in contributing to generate the optimal array of stimuli for driving the cell fate. Nevertheless, the differentiating potential of many other factors remains neglected. In the particular, the effects of gaseous signalling molecules, such as hydrogen sulfide (H_2S), on adult stem cells remain to be investigated. Hydrogen sulfide is an endogenously produced biological agent belonging to the *gasotransmitters* family. H_2S plays pivotal roles in the central nervous, respiratory and cardiovascular systems, where it exerts relevant protective

Peer-reviewed version available at Int. J. Mol. Sci. 2018, 19, 2368; doi:10.3390/ijms19082368

effects. Therefore, H_2S-donors have acquired a great therapeutic potential for widely diffused pathologies, such as neurodegenerative [1-3], cardiovascular [4-6] and gastrointestinal diseases [7,8]. Moreover, their H_2S-release can also be prolonged and potentiated by biological thiols that are normally present in the biological systems such as: protein-thiols groups, cysteine and glutathione (GSH). Endogenously, H_2S is produced in mammalian tissues from L-cysteine or polysulfides metabolism [9]. In particular, the metabolism of organosulfur compounds (OSCs) derived from garlic leads to the production of H_2S slow-releasing donors with antimicrobial, antioxidant [10,11] and anti-inflammatory properties [12] with heart protection, chemo-sensitization features and *in vitro* inhibition of tumour cells proliferation through the induction of apoptosis [12]. On this basis, the garlic OSCs can be considered promising biomolecules to provide antimicrobial/antioxidant properties to scaffolding materials able to support the stem cell differentiation, improving their biological responsiveness in tissue repair and regeneration.

The fabrication of bioactive materials able to fulfil a double function, playing both support and stimulation of the biochemical processes by releasing of signalling molecules, represents a novel approach in the scaffolds production. The H_2S-releasing material could exert a wide range of protective actions, vasodilation, angiogenesis, antioxidant and anti-inflammatory effects, improving the regenerative capacity of tissue engineering grafts, especially in cardiovascular systems [13-16]. Recently, it was demonstrated that H_2S-functionalized hydrogels and fibers are able to enhance the proliferation of human cardiac progenitor/stem cells [17], cardiomyocytes and immortalized fibroblast cell lines [18], and to improve the wound healing process [19].

Fibrous structures are able to mimic the tissue extracellular matrix (ECM) morphology and are very suitable to entrap and stabilize thermo-labile substances, occurring at room temperature and ensuring their controlled release. Nanofibers can be easily obtained by electrospinning technique, which is a low-cost, user friendly and versatile process. Moreover, it allows to process different kinds of materials in fibers, obtaining fibrous structures with diameters ranging from nanometers to microns and large surface area-to-volume ratio [12,20-22]. Among the different biopolymers, poly(lactic) acid (PLA) is widely used, since it is a FDA approved biocompatible and biodegradable polymer with a high hydrophobicity and linear structure that confer excellent spinnability for fabrication of fibrous biomats by electrospinning technique.

Therefore, in this work, two different approaches were used in order to generate electrospun PLA fibrous membranes (PFM) able to provide H_2S slow-release: i) the direct doping of PFM with natural garlic OSCs by drop casting garlic oil-soluble extract (GaOS) on the surface of neat fibrous mats and ii) the optimization of a protocol for the "*ex novo*" production of OSCs-functionalized fibers, by OSCs direct encapsulation within PFM, using both GaOS and diallyl disulfide (DADS). GaOS doped PFMs were here characterized and analyzed for their H_2S-release ability and for their effect on *in vitro* cell proliferation of human cardiac mesenchymal stem cells (cMSC). Moreover, PFM functionalized with GaOS and DADS were produced using a novel protocol for their synthesis and characterized for their morphological, thermal, mechanical and biological properties. The data here presented show that the produced H_2S-releasing fibers can be useful for the optimization of nano-structured patches for tissue repair.

2. Results and Discussion

This section may be divided by subheadings. It should provide a concise and precise description of the experimental results, their interpretation as well as the experimental conclusions that can be drawn.

2.1. GaOS extract production and characterization

GaOS was obtained using a previously optimized extraction protocol [23]. It was characterized by the first step of extraction of the water-soluble fraction at low temperature in order to reduce oxidative reactions. The obtained ethanol-soluble fraction (GaOS) was filtered, analyzed by RP-HPLC (Figure 1A) and stored at -20°C. About 2 ml of GaOS solution, with a concentration of 42 mg of d.w./ml, were obtained for each extraction from 5 g of garlic. The RP-HPLC analysis of the GaOS, shown in Figure 1a, indicated the presence of a main hydrophobic component (corresponding to the peaks a and b), eluted at the same retention time of DADS (see S2 Figure), which represents the major constituent (about the 60%) of the oil-garlic fraction [24]. Garlic OSCs and their conjugates have been studied as optimal H_2S slow-releasing donors [23,25-27]. Therefore, the ability of the GaOS solution to release H_2S was here assessed by MB assay after 30 min, 2 h and 5 h of incubation at 37°C (Figure 1B).

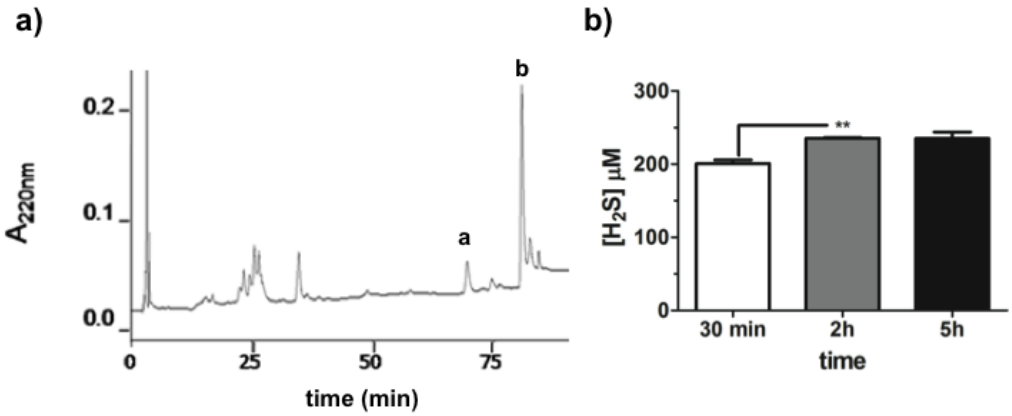

Figure 1. Characterization of the GaOS extract. (**a**) RP-HPLC chromatogram of the GaOS obtained using C_{18} column at 0.8 ml/min flow rate. The elution was performed with a linear gradient of solv. B (80%CH_3CN, 0.1% TFA). Peaks a and b are characteristic of DADS; (**b**) H_2S-release by 25 µL of GaOS after 30 min, 2 h and 5 h of incubation at 37°C in the presence of 1 mM DTT and detected by MB assay.

In particular, the H_2S was released in a time dependent manner, and 25 µL of GaOS led to a production of 200.8± 8.33 µM (±SD) of H_2S after 30 min of incubation at 37°C. This result was in agreement with the already studied property of the garlic OSCs to generate H_2S with a slow-releasing rate [9]. Therefore, for this property and its easy production, GaOS could be of potential interest for the production of biocompatible systems for the H_2S controlled release in therapeutic applications. Indeed, although the pharmacological properties of this *gasotransmitter* have been established, its administration is not easy and is greatly limited by the difficulty of ensuring an accurate posology control and the risk of overdose. On this contest, here we fabricated biocompatible and biodegradable PFM able to embed GaOS and allow a more controlled H_2S slow-release.

2.2. Synthesis of GaOS doped PFM as H_2S-releasing and antimicrobial fibrous-mats

In the last years, there has been a growing interest towards plant oil-extracts with biological activity and the production of related delivery systems for several applications [28-38]. Among them, electrospun fibrous mats have attracted a lot of attention, being ideal for trapping and stabilizing bioactive molecules at room temperature, providing a slow-release of organic molecules and volatile compounds.

In the Figure 2A the SEM micrographs of the neat PFM are shown, evidencing the presence of defect-free randomly oriented fibers with an average diameter of 0.71±0.18 µm (Table 1).

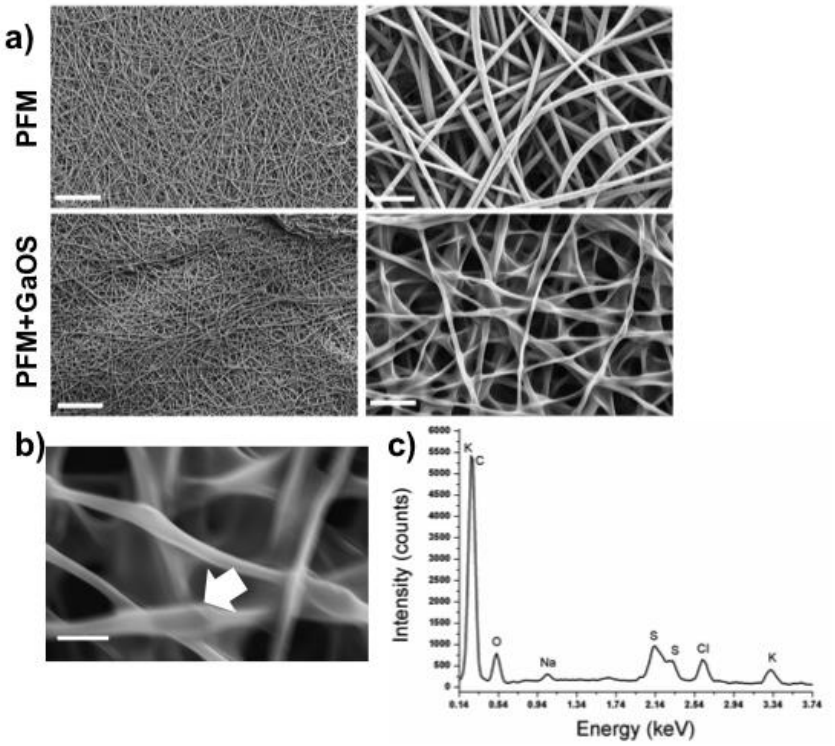

Figure 2. Microstructural characterization of the neat and GaOS doped PFM. (**a**) SEM micrographs of PFM and PFM+GaOS (left: magnification 1kx, scale bar 50 μm, right: magnification 10kx, scale bar 5 μm); (**b**) SEM micrograph (magnification 30kx, scale bar 2μm) and (**c**) EDS spectrum of PFM+GaOS. The white arrow indicates the area submitted to the EDS microanalysis.

The PFM were doped with GaOS (PMF+GaOS) and the GaOS addition slightly modified the fiber morphology, leading to thinner fibers and, consequently, higher fibers packing density (Figures 2A and 2B). Furthermore, the energy dispersive X-ray (EDS) spectrum of the PMF+GaOS, acquired after about 3 weeks from the doping and without special storage, demonstrated the presence of OSCs embedded within the PFM porous network, via detection of sulfur (Figure 2C) that was not presence in the EDS of PFM without GaOS (S3 Figure). These results confirmed a great compatibility between the PFM and the OSCs, guaranteeing a good OSCs adhesion and entrapment between the fibers. Therefore, the H_2S release from the GaOS conditioned PFM was investigated by MB assay. The doped PFM were able to release H_2S in a concentration dependent manner, as shown in the Figure 3A.

Peer-reviewed version available at Int. J. Mol. Sci. 2018, 19, 2368; doi:10.3390/ijms19082368

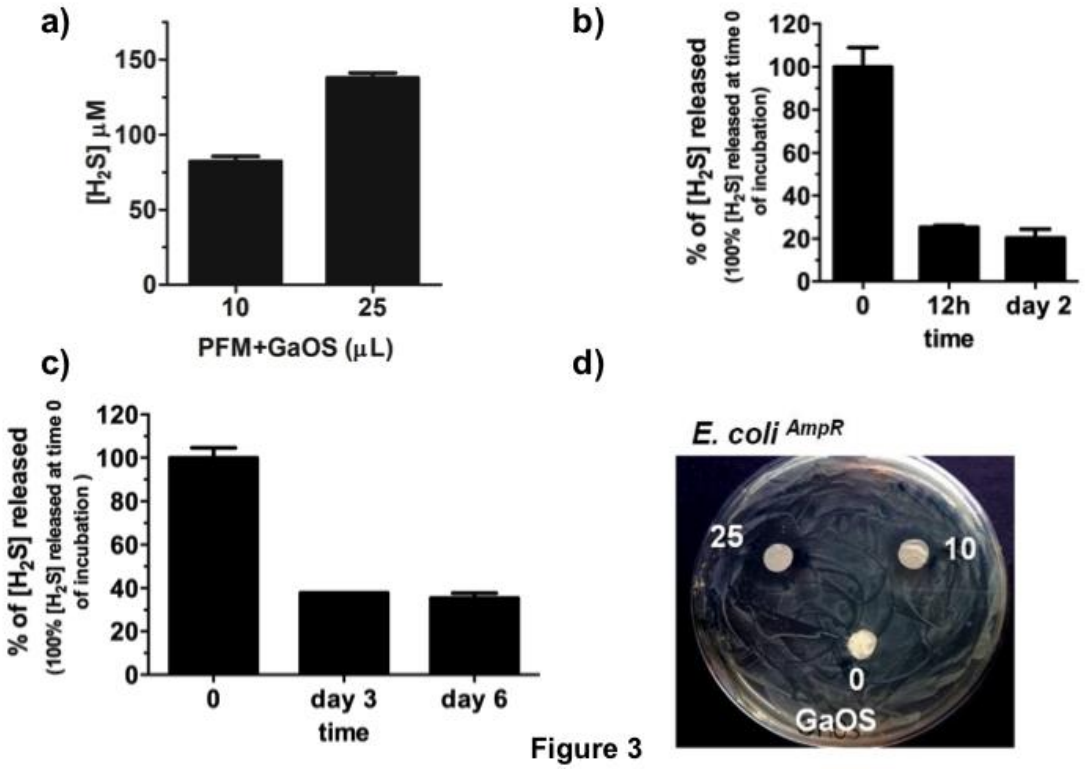

Figure 3

Figure 3. H_2S slow-release and antimicrobial activity of PFM+GaOS. (**a**) H_2S-release by PFM doped with 10 and 25 µL of GaOS; the values of the PFM alone were subtracted. H_2S-release over the time by PFM+GaOS, doped with 25 µL of GaOS after incubation: (**b**) in 50 mM Tris-HCl buffer, pH 8.0 for 0, 12h, 2 days; (**c**) dried in a petri dish at 25°C for 0, 3 and 6 days; (**d**) Photo-optical image of the *E. coli*^{AmpR} growth in agar-LB medium in the presence of PFM disks (1 cm diameter) doped with 0, 10, 25 µL of GaOS (42 mg/ml).

The production of H_2S was 137.8±3.3 µM after 1h shaking at 37°C (±SD), which was little less than that obtained by the GaOS solution after 30 min, even demonstrating that the PFM got a high ability to embed the GaOS extract. The H_2S release from the PFM+GaOS was also performed over the time both after incubation at 37°C in the buffer for 0, 12h and 2 days, and after 0, 3 and 7 days putting them in a petri dish at room temperature. After 2 days of incubation in buffer the membranes were able to release the 20.39 % of the H_2S, while after 6 days the dried PFM+GaOS were able to release the 35.44% of the H_2S produced immediately after doping. These results are in agreement with the demonstrated trapping ability of fibrous membranes, and demonstrate that the H_2S slow-release can be improved embedding the GaOS into the PFM.

Furthermore, since the demonstrated antimicrobial properties of the garlic extracts could represent a key feature for preventing microorganism colonisation and biofilm formation [39], the antibacterial behaviour of the PFM+GaOS was here investigated. The doped PFM were able to inhibit the proliferation of the BL21 *E.coli*^{AmpR} strain in a concentration dependent manner, as it was observable from the absence of the biofilm around the GaOS doped PFM disk (Figure 3D).

Therefore, H_2S-relasing mats with antimicrobial properties, such as GaOS doped PFM, could disclose attractive pharmacological perspectives also in tissue repair and regeneration. In general, the effects of H_2S-donors on stem cells have not been widely investigated yet, and even more the effects of H_2S slow-releasing biomats [17-19,40]. In this contest, the influence of the H_2S-releasing PFM on the adult stem cells was here assessed.

2.3. GaOS doped PFM improve the cMSC proliferation

The PFM+GaOS disks were employed as scaffolds for 2D cultures of Lin$^-$Sca1$^+$ cMSC in order to investigate their effect on the stem cell viability and proliferation. After 3 days of growth, the cell viability of cMSC seeded onto the PFM+GaOS with low concentration of GaOS (4.2 μg d.w.) was increased with respect to the cells seeded on neat PFM (Figure 4A).

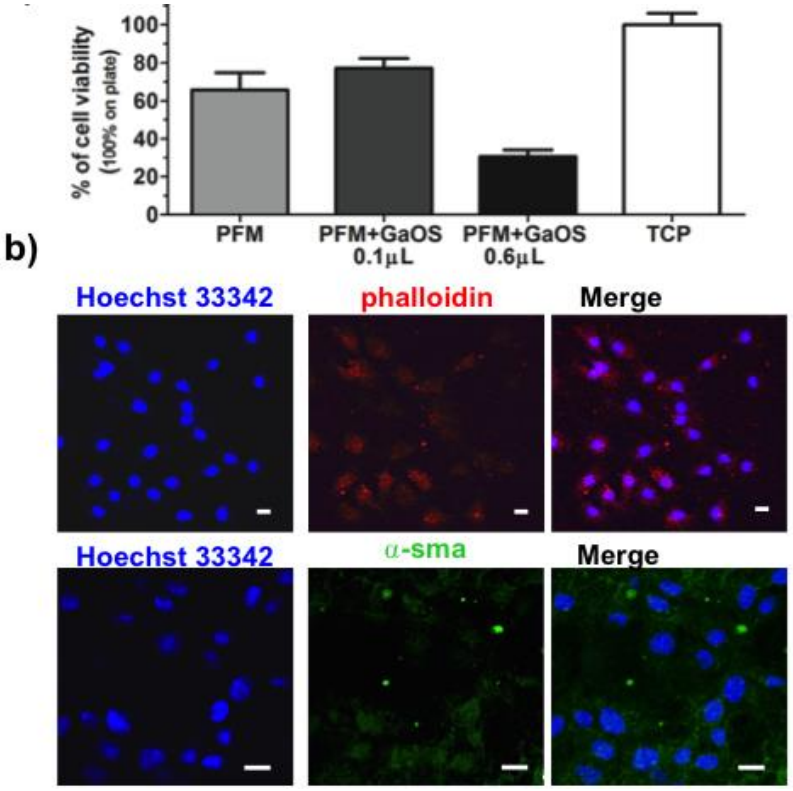

Figure 4. PFM+GaOS as scaffolds for cMSC cultures. (**a**) Cell viability of cMSC seeded on PFM disks (0.5 cm of diameter) with 0, 0.1 and 0.6 μL of GaOS after 3 days of growth; (**b**) Fluorescence confocal micrographs of cMSC cultured on PFM+GaOS for 3 days. The nuclei are stained with Hoeschst 33342 (in blue) and the expressions of α-sma (in green) and phalloidin (in red) proteins are detected. Scale bars= 10 μm.

The results were expressed as a percentage of the control, represented by cells growth on a tissue culture plate (TCP). Figure 4B shows the fluorescence micrographs of cMSC cultured on PFM+GaOS after 3 days of growth; the nuclei and the cytoskeleton were stained with Hoechst and phalloidin respectively. The cells were dispersed on the membrane and a significant production of α-smooth muscle actin (α–sma) was observed, indicating a favourable interaction between the cells and the functionalized biomaterial. By contrast, a cytotoxic effect was revealed using PFM doped with a higher concentration of GaOS (25.2 μg d.w.). These results are in agreement with the effects of the H_2S on the cell growth described in the literature [18]. Indeed, although the exogenous administration of H_2S elicits a wide range of protective effects including anti-inflammatory, antioxidant and down regulation of under stress cellular metabolism, [13,16] by contrast the direct contact with high levels of exogenous H_2S can induce cytotoxicity [18,19].

In order to better clarify the effects of the PFM+GaOS and their *gasotransmitter* releasing ability on cell proliferation of cMSC, other experiments were performed without a direct contact of the PFM with the cells. PFM, with and without 25 μL of a diluted GaOS solution (19.8 mg of d.w./ml) releasing 95 μM of H_2S, were placed to the centre of the lids of petri dishes where 10000 cells/cm^2 were seeded, as shown in the photo-optical image in Figure 5A. After 24h of cell growth, a high increase of the proliferation in the presence of PFM+GaOS was observed, as shown in Figure 5B, where the cMSC

Peer-reviewed version available at Int. J. Mol. Sci. 2018, 19, 2368; doi:10.3390/ijms19082368

were fixed and stained with crystal violet. Accordingly, a statistically significant increase of the cell viability was also observed in the presence of PFM+GaOS by means of MTT assay (Figure 5C). In order to compare the effect of the PFM+GaOS with the PFM embedding a pure and fast H_2S-releasing agent, the cell growth was assessed in the presence of PFM doped with 25 µL of 95 µM Na_2S. Na_2S was immediately released from PFM as H_2S. Also in this last case a significant increase of the cell growth with respect to the absence of H_2S-donors was observed in the absence of H_2O_2 (Figure 5C).

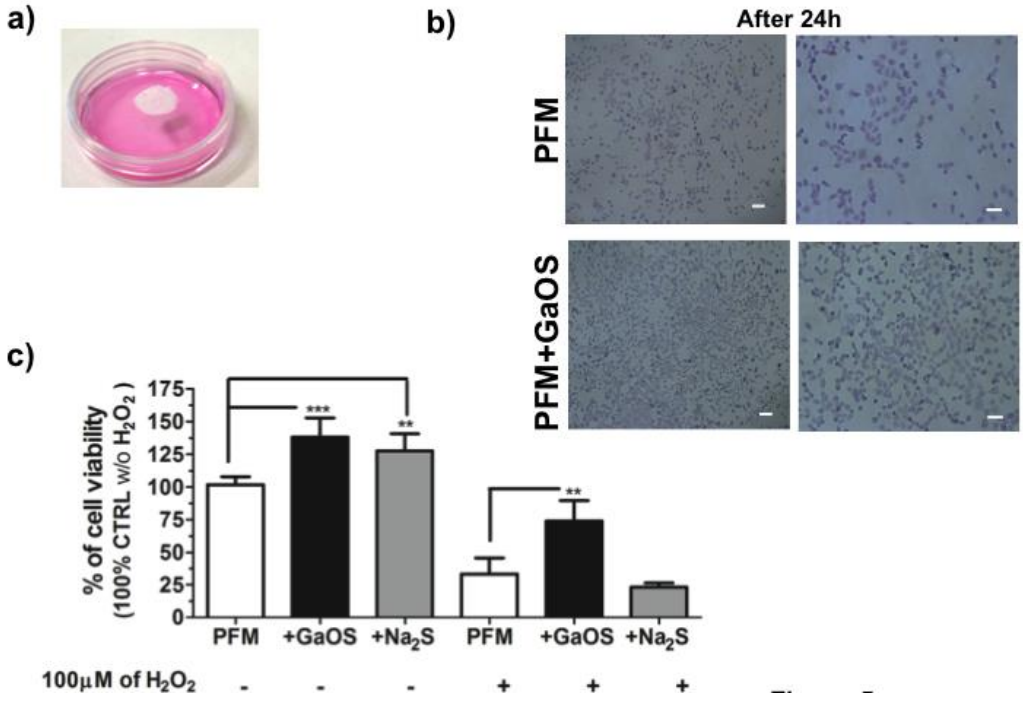

Figure 5. Effect of gaseous release from PFM+GaOS on 2D-culture of cMSC. (**a**) Photo-optical image of PFM+GaOS on the lids of the petri dishes where 1x10^{4}cells/cm^2 were seeded; (**b**) Optical micrographs of cMSC after 24h of cell growth in the presence of PFM+GaOS disk (1 cm of diameter) on the petri dishes-lid and stained with crystal violet; (**c**) Cell viability of cMSC cultures in the presence or in the absence of 100 µM H_2O_2 with PFM, PFM+GaOS or PFM+Na_2S on the petri dishes-lids.

These results indicated that H_2S-releasing PFM+GaOS stimulated the cMSC proliferation through the release of gas molecules and without a direct contact with the cells.

The more stimulating effect of the PFM+GaOS on cell growth respect to the PFM+Na_2S could be related to several factors, such as: i) a slower H_2S-production from the sulfane sulfur compounds present in the garlic extract, that is dependent from hydrolysis or nucleophilic substitution [26]; ii) a better trapping into the fibres of GaOS, due to its hydrophobicity; iii) possible additional H_2S independent pathways.

Moreover, taking into account the ability of H_2S-releasing donors to reduce the cellular oxidative damages [41], the effect of PFM+GaOS on cell growth in the presence of 100 µM H_2O_2 in the cell culture medium was also here assessed. After 24h of cell growth in the presence of 100 µM H_2O_2, we observed a decrease of about 68% of the cell viability in the presence of neat PFM (as control), while only about a 27% of decrease occurred in the presence of PFM+GaOS (Figure 5C). Therefore, the cellular protection from oxidative stress was a peculiarity of PFM+GaOS, which was not obtained in the presence of PFM+Na_2S, where a decrease of about 78% of cell viability was observed (Figure 5C). These results were in agreement with the property of the garlic OSCs to perform a prolonged and gradual H_2S release over the time, which was not obtainable using Na_2S. The prolonged H_2S slow-release most likely leads to an antioxidant protective effect on cells, thereby stimulating cell growth. However, it was not possible to completely exclude that the effect was also due to the formation of other gaseous species able to reduce the oxidative hydrogen peroxide. A previous study on H_2S-releasing poly(ε-

caprolactone) (PCL) fibers [18] demonstrated that the H_2S release induced an anti-proliferative and synergistic effect with H_2O_2 on H9c2 cardiomyoblasts in the absence of cysteine in the cell culture medium. By contrast, in our case a stimulating effect of the PFM+GaOS on the cell proliferation was observed also in the absence of cysteine, probably due to several factors, including the intrinsic properties of the used H_2S-agent and the ability of PLA fibers to release the *gasotransmitter*. Our results on the cyto-protective activity of H_2S-releasing fibrous mats are also in agreement with other recent studies on different H_2S-releasing fibers [19,40] that were able to promote wound healing *in vivo* through cyto-protection. This property was likely due to the ability of the H_2S to reduce the inflammatory response and the oxidative damage, and to stimulate the angiogenesis [55]. Therefore, H_2S-releasing mats, like the H_2S-releasing molecules [41-43], may promptly scavenge hydrogen peroxide, inducing higher intracellular levels of reduced glutathione (GSH), increasing pro-cell survival signalling and, at the same time, decreasing pro-apoptotic signalling. The protective effect of the H_2S-releasing PFM from oxidative damage, which was observed in the non-direct growth on the membranes, opens new perspectives in their application as biomedical devices that could be used inside or outside the body, such as non-implantable devices/patches for wound dressing, implantable material like vascular grafts, heart valves and implants for reducing the ischemic damages and improving the health and medical condition of the patient. Moreover, the enhancing of the wound healing induced by *Allium sativum* L. via re-epithelialization and neovascularization has been already demonstrated [56,57].

2.4. Microstructural and mechanical properties of GaOS and DADS functionalized PFM

An *ex-novo* synthesis of functionalized PFM with encapsulation of GaOS or DADS, as pure garlic OSC, was here performed. In Figure 6, SEM micrographs of the functionalised PFM are compared. In all cases, defect-free randomly oriented fibers were obtained and characterised by a uniform distribution of the OSCs within the fibers, and crystals were not detected within the fibers and on their surface.

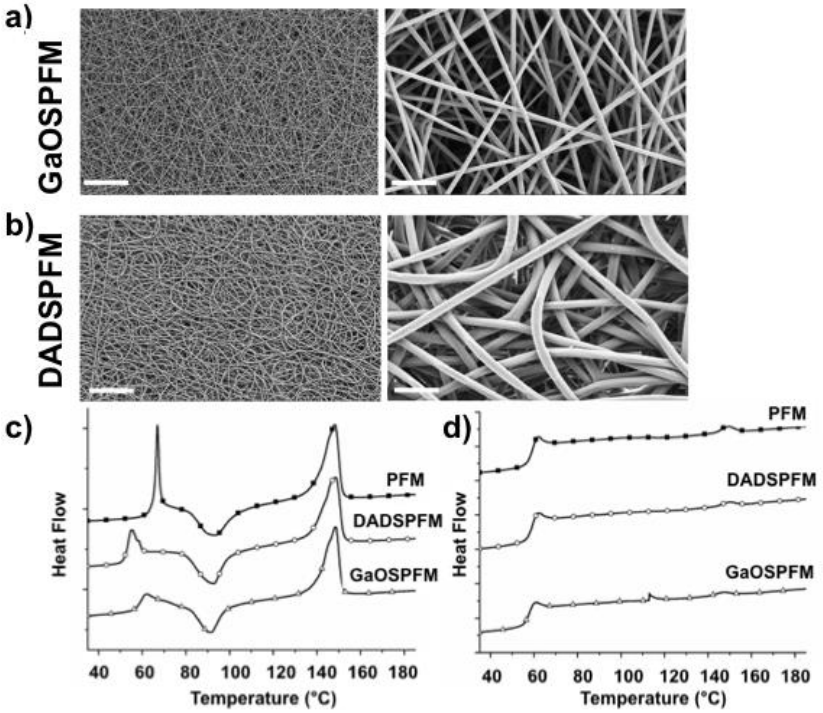

Figure 6. Microstructural and thermal characterization of functionalized PFM. SEM micrographs of (**a**) GaOSPFM and (**b**) DADSPFM (left: magnification 1kx, scale bar 50 μm, right: magnification 10kx, scale bar 5 μm); DSC curves related to the first (**c**) and second (**d**) heating scans of PFM, DADSPFM and GaOSPFM.

The presence of DADS led to bigger fibers (DADSPFM, Figure 6B), with an average diameter of 1.21±0.16 μm (Table 1), than both PFM (average diameter of 0.71±0.18 μm, Table 1, Figure 2A) and GaOSPFM (average diameter of 0.65±0.10 μm) (Table 1, Figure 6A). Moreover, the DADS addition favoured the deposition of more rounded fibers (Figure 6B), whereas the GaOS functionalization did not alter the fiber morphology (Figure 6A), resulting very similar to PFM (Figure 2A).

These results were in agreement with previous studies on the production of PCL fibers loaded with the H_2S donor N-(benzoylthio)benzamide (NSHD1) [18,19]. However, in that case the NSHD1 addition to PCL solutions during the synthesis did not influence the morphology and the average diameter of the PCL fibers [18,19]. On the contrary we evidenced significant differences between PFM and DADSPFM, as described above, suggesting an interaction between DADS and PLA. Moreover, DSC analyses were performed on the PFM, in order to investigate the influence of GaOS and DADS on the thermal properties of the produced fibers. The glass transition (T_g), melting (T_m), cold crystallisation (T_{cc}) temperatures, the melting (ΔH_m) and cold crystallization (ΔH_{cc}) enthalpies and the crystallinity degree (χ), related to the first and the second heating scans, are summarised in Table 1.

Table 1. Average diameter values and mechanical properties of the produced neat and functionalized PFM.

Sample	Average diameter (μm)	E (MPa)	σ_{max} (MPa)	σ_y (MPa)	ε_{max}
PFM	0.71 ± 0.18	28 ± 1	1.1 ± 0.1	0.63 ± 0.01	1.0 ± 0.2
GaOSPFM	0.65 ± 0.10	52 ± 6	2.7 ± 0.3	1.5 ± 0.1	1.0± 0.2
DADSPFM	1.21 ± .0.16	65 ± 18	2.4 ± 0.2	1.6 ± 0.3	1.3 ± 0.1

The first and second heating scan DSC curves are compared in Figure 6C and 6D, respectively. By comparison of the first heating scans data in Table 2, the OSCs addition did not significantly influence the melting temperature (T_{mI}).

Indeed, in all cases, it was possible to detect two melting peaks in the first heating scan DSC curves: a first very broad little shoulder (T_{m1I}), followed by a well-defined melting temperature (T_{m2I}), due to the coexistence of two PLA crystalline structures [44,45] or due to the dual lamellae population. [45]

In details, the lower melting shoulder is ascribed to the crystals formed through a melt-recrystallization process during the heating scan (cold crystallization process), whereas the higher well defined one is associated to the melting of the original crystals derived from the sample preparation [44,45]. On the contrary, OSCs addition led to a significant decrease of T_g value, particularly in the case of DADSPFM, suggesting an interaction between the OSCs and the PLA chains, and a plasticizing effect of the OSCs.

Table 2. Differential scanning calorimetry (DSC) data for PFM, GaOSPFM and DADSPFM.

	I heating						
	T_{gI} (°C)	T_{ccI} (°C)	ΔH_{ccI}(J/g)	T_{m1I} (°C)	T_{m2I} (°C)	ΔH_{mI}(J/g)	χ_I (%)
PFM	65.9	94.04	19.19	145.9	148.8	26.47	7.83
GaOSPFM	59.6	91.54	14.93	145.4	148.4	25.49	11.35
DADSPFM	53.5	92.67	18.21	146.3	148.6	26.08	8.46
	II heating						
	T_{gII} (°C)	T_{ccII} (°C)	ΔH_{ccII} (J/g)	T_{m1I} (°C)	T_{m2II} (°C)	ΔH_{mII} (J/g)	χ_{II} (%)
PFM	59.2	-	-	-	149.8	1.10	1.18
GaOSPFM	58.1	-	-	-	146.8	0.76	0.82
DADSPFM	59.0	-	-	-	149.7	0.73	0.78

Moreover, plasticizers are able to increase polymer chain mobility and flexibility by decreasing intermolecular forces [46] and hydrogen bonding between polymer chains [47,48]. In this manner, the plasticizers presence also tends to promote the cold crystallization process, as testified by the slightly lower T_{cc} values detected for GaOSPFM (91°C) and DADSPFM (92°C) with respect to PFM one (94°C). Indeed, the exothermic peak at around 91-94°C was ascribed to the PLA typical cold crystallization (T_{cc}), characterised by the reorganization of amorphous domains into crystalline regions, promoted by the increased macromolecular flexibility and mobility upon increasing temperature. Thus, the promoted crystallization led to higher crystallinity degree values in the case of OSCs functionalised fibers (Table 2), particularly for GaOSPFM (11.35 % for GaOSPFM *vs.* 7.83 % for PFM). In all cases, the electrospun mats are generally characterised by very low crystallinity degree values, since the electrospinning process favours a rapid evaporation of the solvent and, thus, a fast solidification of stretched chains during the later stages of the process, due to the high elongation strain rate of the electrospinning jet. Consequently, the stretched chains do not have enough time to reorganize before the solidification [49] and the majority of the chains are in the amorphous state. As far as the second heating scan data were concerned, interestingly the glass transition values were very comparable, the cold crystallization phenomenon was not revealed, and the melting was hardly detectable, indicating that, in these samples, the applied cooling conditions were not able to induce the complete PLA crystallization. Moreover, as expected, significantly lower crystallinity degree values were obtained in all cases, due to the elimination of the thermal history, particularly of the influence of the applied process for the production of the fibers and of the fibrous structure, in agreement with previous studies [22,50,51]. Furthermore, the influence of the added OSCs on the mechanical properties of the obtained fibers was studied by means of tensile tests. The stress-strain curves of neat and functionalised PFM are compared in Figure 7A and the data of the uniaxial tensile tests, in terms of ultimate tensile stress (σ_{max}), yield stress (σ_s) and Young's modulus (E), are reported in Table 1.

A remarkably significant increment of the mechanical properties, in terms of Young modulus (E) and σ_{max} (Table 1), was recorded in the case of functionalized PFM with respect to neat PFM (E=28±1 MPa and σ_{max}=1.1±0.1 MPa): E=65±18 MPa and σ_{max}=2.4±0.2 MPa for DADSPFM; E=52±6 MPa and σ_{max}=2.7±0.3 MPa for GaOSPFM. It has to be taken into account that the mechanical properties of electrospun mats are strongly influenced by several factors that interact each other: (i) intrinsic characteristics of the polymer which influence the fibers deformation mechanisms (whose increment causes a higher ultimate tensile stress); (ii) fibers packing density, interaction and mechanical interlocking that increment the elastic modulus; (iii) fibers average diameter size (thinner fibers

correspond to a higher packing density); (iv) possible presence of defects (e.g. beads) in the fibers [21,52].

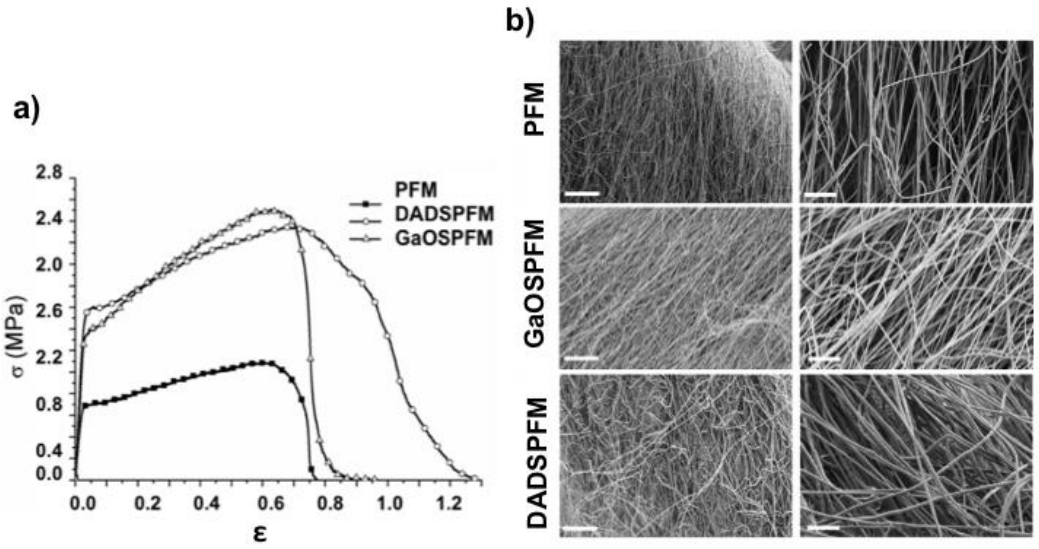

Figure 7. Mechanical properties of functionalized PFM. (**a**) Stress-strain curves of PFM, GaOSPFM and DADSPFM; (**b**) SEM micrographs of the related fracture stress-strained surfaces (left: magnification 1kx, scale bar 50 μm, right: magnification 5kx, scale bar 10 μm).

Moreover, by comparing the SEM micrographs of the stress-strained functionalized PFM surfaces (Figure 7B), the neat PFM and GaOSPFM presented comparable behaviour, with tendency of the fibers to align in the load direction. On the contrary, DADSPFM showed lower fiber alignment degree, due to its different morphological features (Figure 6) with respect to PFM and GaOSPFM. Thus, it is possible to conclude that among the several factors able to simultaneously affect the mechanical behaviour of fibrous mats, the predominant one seems to be the different chemical composition, suggesting an interaction between the sulphur compounds and the polymeric chains, in agreement with DSC data, that evidenced an increased crystallinity degree in the case of functionalized PFM (Table 2). Indeed, improved mechanical properties were revealed for both OSCs functionalised fibers, even if GaOSPFM resulted morphologically comparable to neat PFM (Figures 2A and 6A), presenting comparable average diameter size (Table 1) and, thus, the same interweave degree.

2.5. Biological properties of GaOS and DADS functionalized PFM

The H_2S-releasing properties of GaOSPFM and DADSPFM were assessed and both PFM were able to release H_2S (Figures 8A and B). However, the H_2S-release was very low and less than that observed in the case of PFM doped using 10μl of GaOS. In particular, the release from GaOSPFM was less than that from DADSPFM.

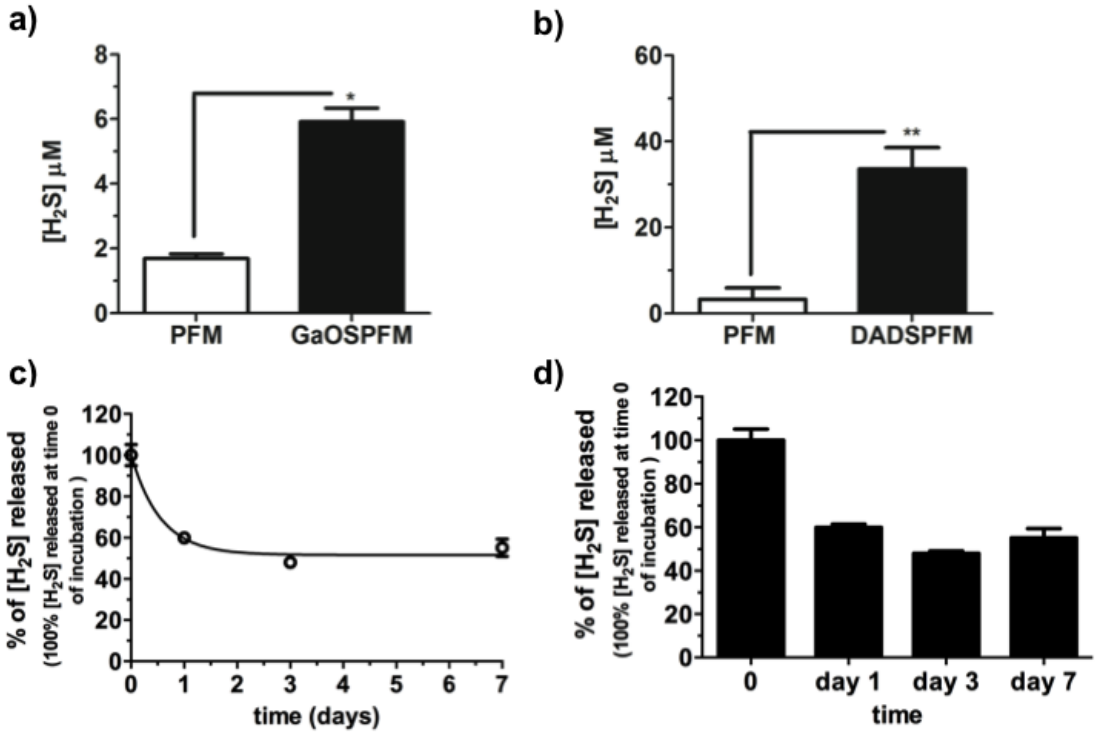

Figure 8. H_2S release of functionalized PFM**.** H_2S release from (**a**) GaOSPFM and (**b**) DADSPFM disks (1 cm of diameter) performed with 1h of incubation at 37°C; H_2S release from DADSPFM disks over the time, after incubation: (**c**) in buffer solution (50 mM Tris HCl, pH 8.0) at 37°C, and (**d**) dried in petri dish at room temperature for 0, 1, 3 and 7 days. *$p < 0.05$.

This result indicated that the concentration of the H_2S-donors was very low in the GaOSPFM, probably due to chemical reactions between the OSCs and the used solvents, which occurred during the PFM synthesis. By contrast, DADSPFM maintained the property to release H_2S even after several days from the synthesis of the fibers (Figure 8B, C and D): after 7 days of incubation in buffer solution the membranes were still able to release 55.19± 4.2% (Figure 8C) of the H_2S produced without incubation, while the 66.39± 6.7% was obtained in dried condition. In this last condition, further, during the first three days, no significant changes in the H_2S release from DADSPFM were observed (Figure 8D).

These data show that the optimized DADSPFM synthesis is able to preserve the DADS properties and to guarantee its controlled release.

In order to assess the potential application of the produced systems as platforms for tissue regeneration, GaOSPFM and DADSPFM were used as scaffolds for 2D-cultures of cMSC (Figure 9). Both the produced PFM did not show a cytotoxic effect and, in particular, the DADSPFM were also able to stimulate the cMSC growth (Figure 9B).

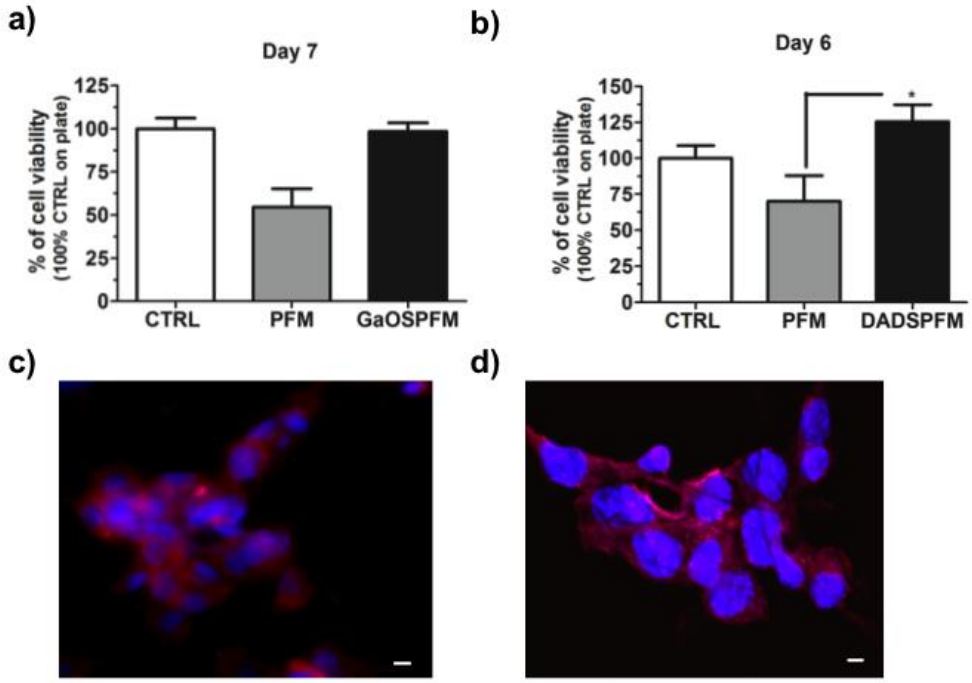

Figure 9. Biological properties of functionalized PFM. Cell viability of cMSC cultured on functionalized PFM: (**a**) on GaOSPFM and (**b**) on DADSPFM after 7 and 6 days of growth, respectively; (**c**) fluorescence micrograph of cMSC seeded on DADSPFM after 6 days and **(d**) confocal micrograph of cMSC seeded on DADSPFM after 7 days of culture. The nuclei are stained with Hoechst 33342 (in blue) and the phalloidin is in red. Scale bars= 10 μm. *$p < 0.02$; ** $p < 0.005$.

The fluorescence micrographs (Figure 9C and D) showed a good adhesion of the cMSC to the DADSPFM and cell-cell interaction after 6 and 7 days of cell culture. These results were also in agreement with our previous studies [17,27], where the hydrogel scaffolds and DADS based nanoemulsions were able to increase the cMSC proliferation and α-sma expression. Therefore, H_2S-relasing fibrous scaffolds might stimulate the tissue repair by activating adult resident stem cells. Moreover, such as previously observed for H_2S-donor molecules [53,54], the DADSPFM could activate the Akt signalling pathways and, thus, could be considered for promoting the endothelial cell growth, migration, wound healing features, capillary morphogenesis and neovascularization of implants.

3. Materials and Methods

.

3.1 Extraction of GaOS from Allium sativum L.

GaOS was prepared as previously described by Buyhan et al. (2015) [23]. Briefly, 5 g of garlic cloves were cut in 50 mM Tris-HCl buffer pH 7.5 at room temperature for about 5-10 min and then the crushing was carried out in liquid N_2 and centrifuged. The precipitated fraction was incubated in absolute EtOH for 24h at room temperature and after centrifugation at 13439 g the ethanol soluble fraction (GaOS) was stored at -20°C. RP-HPLC analysis was performed using mod. LC-10AVP (*Shimadzu, Milan, Italy*), equipped with a C_{18} column (*CPS Analitica,* 150 mmx4.6 mm, 5 μm), using 0.1% trifluoracetic acid as solvent A and 80% CH_3CN, 0.1% trifluoracetic acid as solvent B and with a solvent B gradient (0–5 min, 0%; 5–55 min, 60%; 55–60 min, 60% and 65–85 min 90%). Elute was monitored at 220 nm by UV detector (*Shimadzu, Milan, Italy*).

3.2. PFM synthesis and characterization

3.2.1 Fabrication of doped PFM

Neat PFM were produced by electrospinning. A proper amount of PLA pellets (3051D, *Nature Works*, specific gravity of 1.25 g/cm^3, molecular weight (M_n) of ca. 1.42×10^4 g/mol) (15 % w/v with respect to the used solvents) was dissolved in $CHCl_3$:DMF (67:33, in vol. ratio), under continuous magnetic stirring. The obtained solution was poured in a glass syringe (*Socorex, Switzerland*), equipped with a 18 G needle, fixed in a digitally controlled syringe pump (*KD Scientific, MA, USA*), and electrospun in air at room temperature, setting an applied voltage of 12 kV, a flow rate of 0.5 ml/h and a needle-target distance of 15 cm. The resultant mats were dried under vacuum for 24 h and stored in a desiccator.

Disks (0.5 or 1 cm of diameter) of the produced PFM were cut, sterilized using ethanol and by exposition at UV, and after were doped with GaOS extract by drop casting.

3.2.2.Fabrication of functionalised PFM

OSCs functionalized PFM were prepared by electrospinning technique, using either the GaOS extract or DADS (*Sigma Aldrich, Milan, Italy*). OSCs (5% v/v with respect to the used solvents) and PLA (15 % w/v with respect to the used solvents) based solutions were prepared by dissolving proper amounts of PLA pellets and OSCs in $CHCl_3$:DMF (67:33 v/v). Prepared solutions were poured in a glass syringe, equipped with a 18 G needle, fixed in a digitally controlled syringe pump, and electrospun in air at room temperature, setting an applied voltage of 12 kV, a flow rate of 0.5 ml/h and a needle-target distance of 15 cm.

3.2.3.Characterization of PFM

The morphology of the PFM was investigated by means of field emission gun scanning electron microscopy (*FEG-SEM, Leo Supra 35*), equipped with the energy dispersive X-ray spectroscopy (*EDS, INCA Energy 300, Oxford ELXII detector*). The average fiber diameter was calculated by means of ImageJ (NIH). The thermal properties were measured by differential scanning calorimetry (DSC, *TA Instruments Q2000*) in the following conditions: sample weight ~5 mg, nitrogen flux 50 cc/min, range temperature 0-250 °C, heating and cooling rates 10 °C/min. Melting temperatures (T_{mI} and T_{mII}), cold crystallization temperatures (T_{ccI} and T_{ccII}), melting enthalpies (ΔH_{mI} and ΔH_{mII}), cold crystallization enthalpies (ΔH_{ccI} and ΔH_{ccII}), and crystallinity degrees (χ_I and χ_{II}) were evaluated in the first and in the second heating scans.

The crystallinity degree (χ) was calculated as:

$$\chi = \frac{\Delta H_m - \Delta H_{cc}}{\Delta H_{0,m}} * 100 \quad (1)$$

where ΔH_m, $\Delta H_{0,m}$ and ΔH_{cc} represent the acquired melting enthalpy, the melting enthalpy for 100% crystalline PLA material (i.e. 93 J/g) [58] and the acquired cold crystallization enthalpy, respectively.

Mechanical properties of PFM were investigated by uniaxial tensile tests performed on dog-bone specimens (width 4.8 mm, length 22.25 mm), at 1.2 mm/min to rupture by an electromechanical machine (Lloyd LRX), equipped with a 50 N load cell, following ASTM D882 standard. Four specimens were considered for each electrospun matrix, at least. All mechanical properties were calculated considering the nominal specimen cross-section. Finally, the fracture surface of stress-strained PFM was investigated by means of SEM.

3.3. H_2S releasing assay

The H_2S release from GaOS extract, GaOS doped and OSCs functionalized PFM was estimated by methylene blue (MB) assay, which consists in the reaction between sulfide and N,N-dimethyl-p-phenylenediaminesulphate, in the presence of the oxidizing agent Fe^{3+} in hydrochloric acid, to form methylene blue, involving a 1:2 stoichiometry [23]. Briefly, 25 µl of GaOS solution or PFM based disks (diameter of 1 cm) were incubated in 150 µl of 50 mM Tris HCl, 8.0 pH, buffer and 1 mM of dithiothreitol (DTT) at 37°C for 30 min (in case of the solutions) or 60 min (in case of the PFM). The MB was produced by addition of 20 µl of solution I (20 mM N',N'-dimethyl-p-

phenylenediaminedihydrochloride in 7.2 M HCl) and 20 µl of solution II (30 mM $FeCl_3$ in 1.2 M HCl) and mixing for 10 min at room temperature. The concentration of MB in the supernatants was then spectrophotometrically assessed at 670 nm. The results were plotted using GraphPad Prism version 5.0 for Windows (GraphPad Software, San Diego, CA). The H_2S concentrations were calculated using a calibration curve obtained at different concentrations of Na_2S. Each bar represents the ±SD of three experiments as biological replicas. (S1 Figure)

3.4. Antimicrobial activity

The antimicrobial activity was tested using ampicillin resistant E.coli (E.coli^{AmpR}) BL21 strain grown onto petri dishes with agar-LB medium with 100µg/ml of ampicillin. The disks (diameter of 1 cm) were previously sterilized using ethanol and UV exposure and then were doped with 10 or 25 µl of GaOS extract; the control was performed using 25 µl of ethanol without GaOS. After the evaporation of the solvent, the disks were placed on the petri dishes seeded with the bacteria and incubated at 37°C overnight. The inhibition of the bacterial growth around the disks was analysed.

3.5. Stem cell proliferation on PFM

Cell studies were performed using Lin$^-$ Sca-1^{pos} human cardiac mesenchymal cells (cMSC), which were isolated from human auricular biopsies made during the course of coronary artery bypass surgery and characterized as previously described [59,60]. Cell cultures were performed in Dulbecco's Modified Eagle Medium (DMEM) with high glucose (Gibco, Italy), containing 10% Fetal Bovine Serum (FBS) (Gibco, Italy), 1% penicillin-streptomycin, 1% L-Glutamine-Penicillin-Streptomycin solution (Sigma-Aldrich, Italy).

The biological responsiveness of the produced systems was investigated by in vitro cell viability of cMSC, up to 7 days, using either the methylthiazolyldiphenyl-tetrazolium bromide (MTT) assay [61] or the Water-Soluble Tetrazolium salt (WST-1) assay (4-[3-(4-Iodophenyl)-2-(4-nitrophenyl)-2H-5-tetrazolio]-1,3-benzene disulfonate) (Roche Diagnostics, Sigma Aldrich, Italy) [62].

3.6. Immunofluorescence Analysis

To assess the stem cells phenotype, cMSC were seeded on the PFM scaffolds cultured for 7 days in complete medium. Scaffolds were then washed in PBS, fixed in 4% paraformaldehyde (PFA) in PBS for 15 min at room temperature and permeabilized with 0.2% v/v Triton X-100 (Sigma-Aldrich, Italy) for 10 min. Then they were incubated with antibodies specific for α-smooth muscle actin (α-sma) (Sigma-Aldrich, Italy), followed by the appropriate 488-Alexa fluorochrome-conjugated secondary antibodies (Life Science, Italy), or incubated with 488-Alexa fluorochrome-conjugated phalloidin (Life Science, Italy). Nuclei were stained with Hoechst 33342 (Sigma-Aldrich, Italy). Confocal microscopy of the cell-seeded constructs was performed using a LSM 700 Confocal Laser Scanning Microscope (Carl Zeiss MicroImaging, Jena, Germany) and acquired by means of ZEN 2010 software.

3.7. Statistical analysis

The molecular analysis and cell survival were expressed as mean ± standard deviation (SD). Stem Cell survival was analysed using One-way ANOVA test or the Student's t-test. P values <0.05 were considered significant.

4. Conclusions

New H_2S slow-releasing PFM were here manufactured and characterized for their morphological, thermal, mechanical and biological properties. Two different procedures were used for the production of PFM able to provide H_2S slow-release: i) the direct doping of PFM with natural garlic OSCs by drop casting GaOS on the surface of neat fibrous mats and ii) OSCs direct encapsulation within PFM, using both GaOS and DADS. The produced H_2S-releasing PFM were homogeneous and defect-free with significant increment of the mechanical properties. We show for the first time the capability of the

antimicrobial H_2S-releasing fibers to stimulate the cMSC proliferation were here demonstrated, as well as their ability to reduce the oxidative damage induced by hydrogen peroxide. On this basis, a potential and future application for the PFM+GaOS and DADSPFM could also be for the wound-dressing sector. Moreover, the data here presented suggested the possible exploitation of these low-cost H_2S-releasing fibers as antimicrobial fibrous scaffolds/patches, able to improve the stem cell proliferation and stimulate the tissue regeneration.

Supplementary Materials: Supplementary materials can be found at www.mdpi.com/xxx/s1. **S1 Figure** H_2S slow-releasing by Na_2S and DADS. **A**) Calibration curve of H_2S formation by methylene blue assay, obtained at different concentration of Na_2S by absorbance 670 nm. **B**) H_2S-release at different concentrations of DADS in DMSO, in the presence of 1 mM DTT in 50 mM Tris-HCl, pH 7.4 buffer. The H_2S concentrations were calculated using a calibration curve obtained at different concentrations of Na_2S. Each bar represents the ±SD of three experiments as biological replicas. **S2 Figure** RP-HPLC of DADS. RP-HPLC chromatogram of DADS obtained using C_{18} column at 0.8 ml/min flow rate. The elution was performed with a linear gradient of solv. B (80%CH_3CN, 0.1% TFA). **S3 Figure.** EDS of PFM.

Author Contributions: Conceptualization, S.M. and I.C.; Methodology, I.C., M.C., E.DG.; Investigation, I.C., S.M., M.C., E.DG.; Data Curation, S.M., I.C.; Writing-Original Draft Preparation, S.M.; Writing-Review & Editing, I.C., S.M., M.C., E.DG., F.N.; Visualization, F.N.; Supervision, S.M., I.C.; Project Administration, S.M.; Funding Acquisition, S.M., I.C., F.N.

Funding: This research received no external funding.

Acknowledgments: We thank P. Di Nardo to give us the human cardiac resident MSC line and the association of Italian MAECI, MIUR and CRUI foundation for the Rita Levi Montalcini Award that gave visibility at our scientific work.

Conflicts of Interest: There are no conflicts to declare..

Abbreviations

cMSC	human Lin^- $Sca1^+$ cardiac mesenchymal stem cells
DADS	diallyldisulfide
DADSPFM	poly(lactic) acid fibrous membranes functionalized with DADS
DMF	dimethylformamide
DSC	differential scanning calorimetry
ECM	extracellular matrix
EDS	energy dispersive X-ray spectroscopy
FBS	Fetal Bovine Serum
FEG-SEM	field emission gun scanning electron microscopy
GaOS	garlic oil-soluble extract
GaOSPFM	poly(lactic) acid fibrous membranes functionalized with GaOS
MB	methylene blue
NSHD1	N-(benzoylthio)benzamide
PCL	Polycaprolactone
PFM	poly(lactic) acid fibrous membranes
PLA	poly(lactic) acid
TCP	tissue culture on plate
T_m	melting temperature
α-sma	α-smooth muscle actin
ΔH_m	melting enthalpy
ΔH_{cc}	crystallization enthalpy
χ	crystallinity degree

References

1. Dawe, G. S.; Han, S. P.; Bian, J. S.; Moore, P. K. Hydrogen sulphide in the hypothalamus causes an ATP-sensitive K+ channel-dependent decrease in blood pressure in freely moving rats. *Neuroscience* **2008**, 152, 169-177, DOI: 10.1016/j.neuroscience.2007.12.008
2. Kimura, H. Signaling of hydrogen sulfide and polysulfides. *Antioxid Redox Signal* **2015**, 22, 347-349, DOI: 10.1089/ars.2014.6082
3. Eto, K.; Asada, T.; Arima, K.; Makifuchi, T.; Kimura, H. Brain hydrogen sulfide is severely decreased in Alzheimer's disease. *Biochem Biophys Res Commun* **2002**, 293, 1485-1488, DOI: 10.1016/S0006-291X(02)00422-9
4. Tang, G.; Wu, L.; Liang, W.; Wang, R. Direct stimulation of K(ATP) channels by exogenous and endogenous hydrogen sulfide in vascular smooth muscle cells. *Mol Pharmacol* **2005**, 68, 1757-1764, DOI: 10.1124/mol.105.017467
5. Bucci, M.; Papapetropoulos, A.; Vellecco, V.; Zhou, Z.; Pyriochou, A.; Roussos, C.; Roviezzo, F.; Brancaleone, V.; Cirino, G. Hydrogen sulfide is an endogenous inhibitor of phosphodiesterase activity. *Arterioscler Thromb Vasc Biol* **2010**, 30, 1998-2004, DOI: 10.1161/ATVBAHA.110.209783
6. Sen, U.; Mishra, P. K.; Tyagi, N.; Tyagi, S. C. Homocysteine to hydrogen sulfide or hypertension. *Cell Biochem Biophys* **2010**, 57, 49-58, DOI: 10.1007/s12013-010-9079-y
7. Wallace, J. L. Physiological and pathophysiological roles of hydrogen sulfide in the gastrointestinal tract. *Antioxid Redox Signal* **2010**, 12, 1125-1133, DOI: 10.1089/ars.2009.2900
8. Mard, S. A.; Neisi, N.; Solgi, G.; Hassanpour, M.; Darbor, M.; Maleki, M. Gastroprotective effect of NaHS against mucosal lesions induced by ischemia-reperfusion injury in rat. *Dig Dis Sci* **2012**, 57, 1496-1503, DOI: 10.1007/s10620-012-2051-5
9. Benavides, G. A.; Squadrito, G. L.; Mills, R. W.; Patel, H. D.; Isbell, T. S.; Patel, R. P.; Darley-Usmar, V. M.; Doeller, J. E.; Kraus, D. W. Hydrogen sulfide mediates the vasoactivity of garlic. *Proc Natl Acad Sci U S A* **2007**, 104, 17977-17982, DOI: 10.1073/pnas.0705710104
10. Harris, J. C.; Cottrell, S. L.; Plummer, S.; Lloyd, D. Antimicrobial properties of Allium sativum (garlic). *Appl Microbiol Biotechnol* **2001**, 57, 282-286, DOI: 10.1007/s002530100722
11. Perez-Severiano, F.; Rodriguez-Perez, M.; Pedraza-Chaverri, J.; Maldonado, P. D.; Medina-Campos, O. N.; Ortiz-Plata, A.; Sanchez-Garcia, A.; Villeda-Hernandez, J.; Galvan-Arzate, S.; Aguilera, P.; Santamaria, A. S-Allylcysteine, a garlic-derived antioxidant, ameliorates quinolinic acid-induced neurotoxicity and oxidative damage in rats. *Neurochem Int* **2004**, 45, 1175-1183, DOI: 10.1016/j.neuint.2004.06.008
12. Ramakrishna, S.; Jose, R.; Archana, P. S.; Nair, A. S.; Balamurugan, R.; Venugopal, J.; Teo, W. E. Science and engineering of electrospun nanofibers for advances in clean energy, water filtration, and regenerative medicine. *J Mater Sci* **2010**, 45, 6283-6312, DOI: 10.1007/s10853-010-4509-1
13. Olson, K. R. The therapeutic potential of hydrogen sulfide: separating hype from hope. *Am J Physiol Regul Integr Comp Physiol*, 301, R297-312, DOI: 10.1152/ajpregu.00045.2011
14. Hsiao, S. T.; Dilley, R. J.; Dusting, G. J.; Lim, S. Y. Ischemic preconditioning for cell-based therapy and tissue engineering. *Pharmacol Ther* **2014**, 142, 141-153, DOI: 10.1016/j.pharmthera.2013.12.002
15. Foley, D. P.; Chari, R. S. Ischemia–reperfusion injury in transplantation: novel mechanisms and protective strategies. *Transplant Rev* **2007**, 21, 43-53, DOI: 10.1016/j.trre.2007.01.004
16. Whiteman, M.; Moore, P. K. Hydrogen sulfide and the vasculature: a novel vasculoprotective entity and regulator of nitric oxide bioavailability? *J Cell Mol Med* **2009**, 13, 488-507, DOI: 10.1111/j.1582-4934.2009.00645.x
17. Mauretti, A.; Neri, A.; Kossover, O.; Seliktar, D.; Nardo, P. D.; Melino, S. Design of a Novel Composite H2 S-Releasing Hydrogel for Cardiac Tissue Repair. *Macromol Biosci* **2016**, 16, 847-858, DOI: 10.1002/mabi.201500430
18. Feng, S.; Zhao, Y.; Xian, M.; Wang, Q. Biological thiols-triggered hydrogen sulfide releasing microfibers for tissue engineering applications. *Acta Biomater* **2016**, 27, 205-213, DOI: 10.1016/j.actbio.2015.09.010
19. Wu, J.; Li, Y.; He, C.; Kang, J.; Ye, J.; Xiao, Z.; Zhu, J.; Chen, A.; Feng, S.; Li, X.; Xiao, J.; Xian, M.; Wang, Q. Novel H2S Releasing Nanofibrous Coating for In Vivo Dermal Wound Regeneration. *ACS Appl Mater Interfaces* **2016**, DOI: 10.1021/acsami.6b06466
20. Lagaron, J. M.; Lopez-Rubio, A. Nanotechnology for bioplastics: opportunities, challenges and strategies. *Trends Food Sci Technol* **2011**, 22, 611-617, DOI: 10.1016/j.tifs.2011.01.007

21. Bianco, A.; Calderone, M.; Cacciotti, I. Electrospun PHBV/PEO co-solution blends: microstructure, thermal and mechanical properties. *Mater Sci Eng C* **2013**, 33, 1067-1077, DOI: 10.1016/j.msec. 2012.11.030
22. Cacciotti, I.; Fortunati, E.; Puglia, D.; Kenny, J. M.; Nanni, F. Effect of silver nanoparticles and cellulose nanocrystals on electrospun poly(lactic) acid mats: morphology, thermal properties and mechanical behavior. *Carbohydr Polym* **2014**, 103, 22-31, DOI: 10.1016/j.carbpol.2013.11.052
23. Bhuiyan, A. I.; Papajani, V. T.; Paci, M.; Melino, S. Glutathione-Garlic Sulfur Conjugates: Slow Hydrogen Sulfide Releasing Agents for Therapeutic Applications. *Molecules* **2015**, 20, 1731-1750, DOI: 10.3390/molecules20011731
24. Dausch, J. G.; Nixon, D. W. Garlic: a review of its relationship to malignant disease. *Prev Med* **1990**, 19, 346-361, DOI: 10.1016/0091-7435(90)90034-H
25. Martelli, A.; Testai, L.; Breschi, M. C.; Blandizzi, C.; Virdis, A.; Taddei, S.; Calderone, V. Hydrogen sulphide: novel opportunity for drug discovery. *Med Res Rev* **2012**, 32, 1093-1130, DOI: 10.1002/med.20234
26. Benavides, G. A.; Squadrito, G. L.; Mills, R. W.; Patel, H. D.; Isbell, T. S.; Patel, R. P.; Darley-Usmar, V. M.; Doeller, J. E.; Kraus, D. W. Hydrogen sulfide mediates the vasoactivity of garlic. *Proc Natl Acad Sci U S A* **2007**, 104, 17977-17982, DOI: 10.1073/pnas.0705710104
27. Ciocci, M.; Iorio, E.; Carotenuto, F.; Khashoggi, H. A.; Nanni, F.; Melino, S. H2S-releasing nanoemulsions: a new formulation to inhibit tumor cells proliferation and improve tissue repair. *Oncotarget* **2016**, 7, 84338-84358, DOI: 10.18632/oncotarget.12609
28. Zhang, W.; Huang, C.; Kusmartsev, O.; Thomas, N. L.; Mele, E. Electrospinning of polylactic acid fibres containing tea tree and Manuka. *React Funct Polym* **2017**, 117, 106-111, DOI: 10.1016/j.reactfunctpolym.2017.06.013
29. Rieger, K. A.; Schiffman, J. D. Electrospinning an essential oil: cinnamaldehyde enhances the antimicrobial efficacy of chitosan/poly(ethylene oxide) nanofibers. *Carbohydr Polym* **2014**, 113, 561-568, DOI: 10.1016/j.carbpol.2014.06.075
30. Wen, P.; Zhu, D. H.; Feng, K.; Liu, F. J.; Lou, W. Y.; Li, N.; Zong, M. H.; Wu, H. Fabrication of electrospun polylactic acid nanofilm incorporating cinnamon essential oil/beta-cyclodextrin inclusion complex for antimicrobial packaging. *Food Chem* **2016**, 196, 996-1004, DOI: 10.1016/j.foodchem.2015.10.043
31. Duncan, T. V. Applications of nanotechnology in food packaging and food safety: barrier materials, antimicrobials and sensors. *J Colloid Interface Sci* **2011**, 363, 1-24, DOI: 10.1016/j.jcis.2011.07.017
32. Tartarini, D.; Mele, E. Adult Stem Cell Therapies for Wound Healing: Biomaterials and Computational Models. *Front Bioeng Biotechnol* **2015**, 3, 206, DOI: 10.3389/fbioe.2015.00206.
33. Zhang, W.; Ronca, S.; Mele, E. Electrospun Nanofibres Containing Antimicrobial Plant Extracts. *Nanomaterials (Basel)* **2017**, 7, 42, DOI: 10.3390/nano7020042.
34. Liakos, I.; Rizzello, L.; Hajiali, H.; Brunetti, V.; Carzino, R.; Pompa, P. P.; Athanassiou, A.; Mele, E. Fibrous wound dressings encapsulating essential oils as natural antimicrobialagents. *J Mater Chem B* **2015**, 3, 1583-1589, DOI:10.1039/C4TB01974A
35. Hajiali, H.; Summa, M.; Russo, D.; Armirotti, A.; Brunetti, V.; Bertorelli, R.; Athanassiou, A.; Mele, E. Alginate-lavender nanofibers with antibacterial and anti-inflammatory activity to effectively promote burn healing. *J Mater Chem B* **2016**, 4, 1686-1695, DOI: 10.1039/C5TB02174J
36. Mele, E. Electrospinning of natural polymers for advanced wound care: towards responsive and adaptive dressings. *J Mater Chem B* **2016**, 4, 4801-4812, DOI: 10.1039/C6TB00804F
37. Morsy, R.; Hosny, M.; Reicha, F.; Elnimr, T. Developing a potential antibacterial longterm degradable electrospun gelatin-based composites mats for wound dressing applications. *React Funct Polym* **2017**, 114, 8-12, DOI: 10.1016/j.reactfunctpolym.2017.03.001
38. Lee, C. H.; Chang, S. H.; Chen, W. J.; Hung, K. C.; Lin, Y. H.; Liu, S. J.; Hsieh, M. J.; Pang, J. H. S.; Juang, J. H. J. Augmentation of diabetic wound healing and enhancement of collagen content using nanofibrous glucophage-loaded collagen/PLGA scaffold membranes. *Colloid Interface Sci* **2015**, 439, 88-97, DOI: 10.1016/j.jcis.2014.10.028
39. Tsao, S.; Yin, M. In vitro activity of garlic oil and four diallyl sulphides against antibiotic-resistant Pseudomonas aeruginosa and Klebsiella pneumoniae. *J Antimicrob Chemother* **2001**, 47, 665-670, DOI: 10.1093/jac/47.5.665
40. Sarhan, W. A.; Azzazy, H. M.; El-Sherbiny, I. M. Honey/Chitosan Nanofiber Wound Dressing Enriched with Allium sativum and Cleome droserifolia: Enhanced Antimicrobial and Wound Healing Activity. *ACS Appl Mater Interfaces* **2016**, 8, 6379-6390, DOI: 10.1021/acsami.6b00739

41. Kimura, H. Physiological Roles of Hydrogen Sulfide and Polysulfides. *Handb Exp Pharmacol* **2015**, 230, 61-81, DOI: 10.1007/978-3-319-18144-8_3
42. Pryor, W. A.; Houk, K. N.; Foote, C. S.; Fukuto, J. M.; Ignarro, L. J.; Squadrito, G. L.; Davies, K. J. Free radical biology and medicine: it's a gas, man! *Am J Physiol Regul Integr Comp Physiol* **2006**, 291, R491-511, DOI: 10.1152/ajpregu.00614.2005
43. Ansari, S. B.; Kurian, G. A. Hydrogen sulfide modulates sub-cellular susceptibility to oxidative stress induced by myocardial ischemic reperfusion injury. *Chem Biol Interact* **2016**, 252, 28-35, DOI: 10.1016/j.cbi.2016.03.036
44. Yasuniwa, M.; Tsubakihara, S.; Sugimoto, Y.; Nakafuku, C. Thermal analysis of the double-melting behavior of poly(Llactic acid). *J Polym Sci B* **2004**, 42, 25-32, DOI: 10.1002/polb.10674
45. Radjabian, M.; Kish, M. H.; Mohammadi, N. Characterization of poly(lactic acid) multifilament yarns. I. The structure and thermal behaviour. *J Appl Polym Sci* **2010**, 117, 1516-1525, DOI: 10.1002/app.32046
46. Romera-Bastida, C. A.; Bello-Perez, L. A.; Garcia, M. A.; Martino, M. N.; Solorza-Feria, J.; Zaritzky, N. E. Physicochemical and microstructural characterization of films prepared by thermal and cold gelatinization from non-conventional sources starches. *Carbohydr Polym* **2006**, 60, 235-244, DOI: 10.1016/j.carbpol.2005.01.004
47. Bao, L.; Dorgan, J. R.; Knauss, D.; Hait, S.; Oliveira, N. S.; Marucho, I. M. Gas permeation properties of poly (lactide acid) revisited. *J Memb Sci* **2006**, 285, 166-172, DOI: 10.1016/j.memsci.2006.08.021
48. Mali, S.; Grossmann, M. V. E.; Gracia, M. A.; Martino, M. N.; Zaritzky, N. E. Effects of controlled storage on thermal, mechanical and barrier properties of plasticized films from different starch sources. *J Food Eng* **2006**, 75, 453-460, DOI: 10.1016/j.jfoodeng.2005.04.031
49. Zong, X.; Kim, K.; Fang, D.; Ran, S.; Hsiao, B. S.; Chu, B. Structure and process relationship of electrospun bioabsorbable nanofiber membranes. *Polymer* **2002**, 43, 4403-4460, DOI: 10.1016/S0032-3861(02)00275-6
50. Liu, D.; Yuan, X.; Bhattacharyya, D. The effects of cellulose nanowhiskers on electrospun poly (lactic acid) nanofibres. *J Mater Sci* **2012**, 47, 3159-3165, DOI: 10.1007/s10853- 011-6150-z
51. Bianco, A.; Bozzo, B.M.; Del Gaudio, C.; Cacciotti, I.; Armentano, I.; Dottori, M.; D'Angelo, F.; Martino, S.; Orlacchio, A.; Kenny, J.M. Poly(L-lactic acid)/calcium-deficient nanohydroxyapatite electrospun mats for murine bone marrow stem cell cultures. *J Bioact Compat Pol* **2011**, 26, 225-241, DOI: 10.1177/0883911511406250
52. Li, W. J.; Cooper, J. A., Jr.; Mauck, R. L.; Tuan, R. S. Fabrication and characterization of six electrospun poly(alpha-hydroxy ester)-based fibrous scaffolds for tissue engineering applications. *Acta Biomater* **2006**, 2, 377-385, DOI: 10.1016/j.actbio.2006.02.005
53. Cai, W. J.; Wang, M. J.; Moore, P. K.; Jin, H. M.; Yao, T.; Zhu, Y. C. The novel proangiogenic effect of hydrogen sulfide is dependent on Akt phosphorylation. *Cardiovasc Res* **2007**, 76, 29-40, DOI: 10.1016/j.cardiores.2007.05.026
54. Papapetropoulos, A.; Pyriochou, A.; Altaany, Z.; Yang, G. D.; Marazioti, A.; Zhou, Z. M.; Jeschke, M. G.; Branski, L. K.; Herndon, D. N.; Wang, R.; Szabo, C. Hydrogen sulfide is an endogenous stimulator of angiogenesis. *Proceedings of the National Academy of Sciences of the United States of America* **2009**, 106, 21972-21977, DOI: 10.1073/pnas.0908047106
55. Szabo, C.; Papapetropoulos, A. International Union of Basic and Clinical Pharmacology. CII: Pharmacological Modulation of H_2S Levels: H2S Donors and H2S Biosynthesis Inhibitors. *Pharmacol Rev.* **2017**; 69, 497-564, DOI: 10.1124/pr.117.014050
56. Pazyar, N.; Feily, A. Garlic in dermatology. *Dermatol Reports* **2011**, 3, e4, DOI: 10.4081/dr.2011.e4
57. Sidik, K.; Mahmood, A.; Salmah, I. Acceleration of Wound Healing by Aqueous Extract of Allium sativum in Combination with Honey on Cutaneous Wound Healing in Rats. *Int. J. Mol. Med. Adv. Sci.* **2006**, 2, 231-235, DOI: ijmmas.2006.231.235
58. Riga, A.; Zhang, J.; Collis, J. Characterization of drawn and undrawn polyl-lactide films by differential scanning calorimetry, *Journal of Thermal Analysis and Calorimetry*. **2004**, 75, 257-268, DOI: 10.1023/B:JTAN.0000017347.08469.b1
59. Smits, A. M.; van Vliet, P.; Metz, C. H.; Korfage, T.; Sluijter, J. P.; Doevendans, P. A.; Goumans, M. J. Human cardiomyocyte progenitor cells differentiate into functional mature cardiomyocytes: an in vitro model for studying human cardiac physiology and pathophysiology. *Nat Protoc* **2009**, 4, 232-243, DOI: 10.1038/nprot.2008.229
60. Forte, G.; Pietronave, S.; Nardone, G.; Zamperone, A.; Magnani, E.; Pagliari, S.; Pagliari, F.; Giacinti, C.; Nicoletti, C.; Musaro, A.; Rinaldi, M.; Ribezzo, M.; Comoglio, C.; Traversa, E.; Okano, T.; Minieri, M.; Prat, M.; Di Nardo, P. Human cardiac progenitor cell grafts as unrestricted source of supernumerary cardiac cells in healthy murine hearts. *Stem Cells* **2011**, 29, 2051-2061, DOI: 10.1002/stem.763

61. Denizot, F.; Lang, R. Rapid colorimetric assay for cell growth and survival. Modifications to the tetrazolium dye procedure giving improved sensitivity and reliability. *J Immunol Methods* **1986**, 89, 271-277, DOI: 10.1016/0022-1759(86)90368-6
62. Koyanagi, M.; Kawakabe, S.; Arimura, Y. A comparative study of colorimetric cell proliferation assays in immune cells. *Cytotechnology* **2016**, *68*, 1489-1498, DOI: 10.1007/s10616-015-9909-2

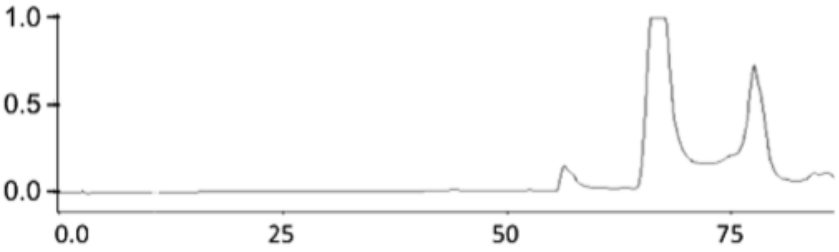

Figure 1S

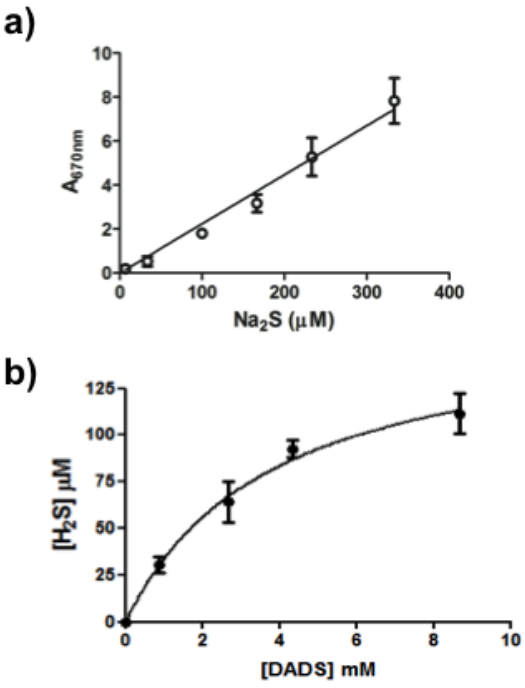

Figure 2S

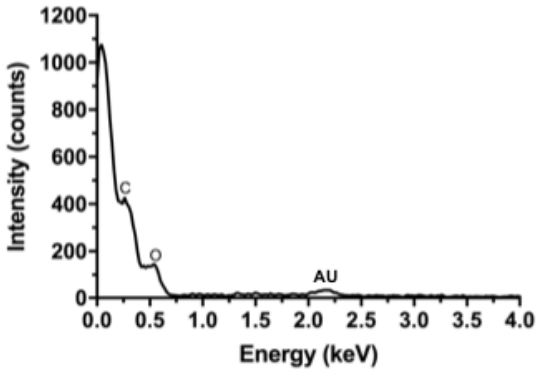

Figure 3S